Geometric Scaling in Inclusive Charm Production

V. P. Gonçalves[1,*] and M. V. T. Machado[1,2,†]

[1]*Instituto de Física e Matemática, Universidade Federal de Pelotas, Caixa Postal 354, CEP 96010-090, Pelotas, RS, Brazil*
[2]*High Energy Physics Phenomenology Group, GFPAE, IF-UFRGS, Caixa Postal 15051, CEP 91501-970, Porto Alegre, RS, Brazil*
(Received 8 July 2003; published 14 November 2003)

We show that the cross section for inclusive charm production exhibits geometric scaling in a large range of photon virtualities. In the DESY ep collider HERA kinematic domain the saturation momentum $Q_{sat}^2(x)$ stays below the hard scale $\mu_c^2 = 4m_c^2$, implying charm production probing mostly the color transparency regime and unitarization effects being almost negligible. We derive our results considering two saturation models which are able to describe the HERA data for the proton structure function at small values of the Bjorken variable x. A striking feature is the scaling on $\tau \equiv Q^2/Q_{sat}^2(x)$ above te saturation limit, corroborating recent theoretical studies.

Introduction.—The behavior of ep or pp scattering in the limit of high center-of-mass energy $\sqrt{s}$ and fixed momentum transfer is one of the outstanding open questions in the theory of the strong interactions. Over the past few years much theoretical effort has been devoted towards the understanding of the growth of the total scattering cross sections with energy. These studies are mainly motivated by the violation of the unitarity (or Froissart) bound by the solutions of the linear perturbative Dokshitzer-Gribov-Lipatov-Altarelli-Parisi (DGLAP) [1] and Balitskiĭ-Fadin-Kuraev-Lipatov (BFKL) [2] evolution equations. Since these evolution equations predict that the cross section rises obeying a power law of the energy, violating the Froissart bound [3], new dynamical effects associated with the unitarity corrections are expected to stop its further growth [4,5]. This expectation can be easily understood: while for large momentum transfer $k_\perp$, the BFKL equation predicts that the mechanism $g \rightarrow gg$ populates the transverse space with a large number of small size gluons per unit of rapidity (the transverse size of a gluon with momentum $k_\perp$ is proportional to $1/k_\perp$), for small $k_\perp$ the produced gluons overlap and fusion processes, $gg \rightarrow g$, are equally important. Considering the latter process, the rise of the gluon distribution below a typical scale is reduced, restoring the unitarity. That typical scale is energy dependent and is called saturation scale Q_{sat}. The saturation momentum sets the critical transverse size for the unitarization of the cross sections. In other words, unitarity is restored by including nonlinear corrections in the evolution equations [4–17]. Such effects are small for $k_\perp^2 > Q_{sat}^2$ and very strong for $k_\perp^2 < Q_{sat}^2$, leading to the saturation of the scattering amplitude. The successful description of all inclusive and diffractive deep inelastic data at the DESY ep collider HERA by saturation models [18–20] suggests that these effects might become important in the energy regime probed by current colliders.

One striking feature of the available saturation approaches is the prediction of the geometric scaling. Namely, the total $\gamma^* p$ cross section at large energies is not a function of the two independent variables x and Q but is rather a function of the single variable $\tau = Q^2/Q_{sat}^2$. As usual, Q^2 is the photon virtuality and x is the Bjorken variable. A current open question is to what extent the geometric scaling is valid above the saturation scale by studying the available high energy formulations for the linear regime. In Ref. [21] the authors have demonstrated that the geometric scaling predicted at low momenta $Q^2 \leq Q_{sat}^2(x)$ is preserved by the BFKL evolution (at both the fixed and running coupling constants) up to relatively large virtualities, within the kinematical window $1 \leq \ln\tau \ll \ln(Q_{sat}^2/\Lambda_{QCD}^2)$. On the other hand, in Ref. [22], the impact of the QCD DGLAP evolution on the geometric scaling has been studied. In this case, the DGLAP evolution equation is solved imposing as initial conditions along the critical line $Q^2 = Q_{sat}^2(x)$ satisfying scaling, showing that it is approximately preserved at very small x. The residual scaling violation is factored out, although the determination of a window for the scaling above Q_{sat} is not provided. As demonstrated in Ref. [23], the DESY ep HERA data on the proton structure function F_2 are consistent with scaling at $x \leq 0.01$ and $Q^2 \leq 400$ GeV^2. Similar behavior has been observed in exclusive [24] and electron-nuclei processes [25]. These results, while not entirely compelling, provide a strong motivation for further investigations.

Here we show that the data on inclusive charm production at the DESY ep HERA exhibit geometric scaling above the saturation scale. Namely, the charm inclusive cross section depends upon $\tau = Q^2/Q_{sat}^2(x)$ alone, where we have taken into account that the saturation scale is given by the saturation model [18]; i.e., $Q_{sat}^2 = (x_0/x)^\lambda$. Moreover, we extend the symmetric saturation model proposed in Ref. [26] for the charm case and derive an analytical expression for the charm production cross section, which explicitly presents geometric scaling. We show that both prescriptions give similar results.

Geometric scaling.—Let us consider the deep inelastic scattering in the dipole frame, in which most of the energy is carried by the hadron, while the virtual photon

γ^* has just enough energy to dissociate into a quark-antiquark pair before the scattering. In this representation the probing projectile fluctuates into a quark-antiquark pair (a dipole) with transverse separation $r_\perp \sim 1/Q$ long after the interaction, which then scatters off the proton. The interaction $\gamma^* p$ is further factorized in the simple formulation [27],

$$\sigma_{L,T}^{\gamma^* p}(x, Q^2) = \int dz d^2 r_\perp |\Psi_{L,T}(z, r_\perp, Q^2)|^2 \sigma_{\text{dip}}(x, r_\perp),$$

where z is the longitudinal momentum fraction of the quark and $x \simeq Q^2/W_{\gamma p}^2$ is equivalent to the Bjorken variable. The photon wave functions $\Psi_{L,T}$ are determined from light cone perturbation theory and read as [27]

$$|\Psi_T|^2 = \frac{6\alpha_{\text{em}}}{4\pi^2} \sum_f e_f^2 \{[z^2 + (1 - z)^2]\varepsilon^2 K_1^2(\varepsilon r_\perp)$$
$$+ m_f^2 K_0^2(\varepsilon r_\perp)\}, \qquad (1)$$
$$|\Psi_L|^2 = \frac{6\alpha_{\text{em}}}{\pi^2} \sum_f e_f^2 \{Q^2 z^2 (1 - z)^2 K_0^2(\varepsilon r_\perp)\},$$

where the auxiliary variable $\varepsilon^2 = z(1 - z) Q^2 + m_f^2$ depends on the quark mass, m_f. The $K_{0,1}$ are the McDonald functions and the summation is performed over the quark flavors.

The dipole hadron cross section σ_{dip} contains all information about the target and the strong interaction physics. In the color glass condensate (CGC) formalism [8,11], σ_{dip} can be computed in the eikonal approximation, resulting in

$$\sigma_{\text{dip}}(x, r_\perp) = 2 \int d^2 b_\perp [1 - S(x, r_\perp, b_\perp)], \qquad (2)$$

where S is the S-matrix element which encodes all the information about the hadronic scattering, and thus about the nonlinear and quantum effects in the hadron wave function. The function S can be obtained by solving an appropriate evolution equation in the rapidity $y \equiv \ln(1/x)$. The main properties of S are (a) for the interaction of a small dipole ($r_\perp \ll 1/Q_{\text{sat}}$), $S(r_\perp) \approx 1$, which characterizes that this system is weakly interacting; (b) for a large dipole ($r_\perp \gg 1/Q_{\text{sat}}$), the system is strongly absorbed which implies $S(r_\perp) \ll 1$. This property is associated to the large density of saturated gluons in the hadron wave function. In our analysis we initially consider the phenomenological saturation model proposed in Ref. [18] which encodes the main properties of the saturation approaches. In this model

$$\frac{\sigma_{\text{dip}}(x, r_\perp)}{\sigma_0} = 1 - S(x, r_\perp); \qquad S = \exp\left[-\frac{Q_{\text{sat}}^2(x) r_\perp^2}{4}\right], \qquad (3)$$

with $\sigma_{\text{dip}}/\sigma_0$ the scattering amplitude, averaged over all impact parameters $b_\perp$, and $Q_{\text{sat}}^2 \simeq \Lambda^2 e^{\lambda \ln(x_0/x)}$. The parameters of the model were constrained from the DESY ep collider HERA small x data, resulting in typical values of order 1–2 GeV^2 for the momentum scale. We

have that when $Q_{\text{sat}}^2(x) r_\perp^2 \ll 1$, the model reduces to color transparency, whereas as one approaches the region $Q_{\text{sat}}^2(x) r_\perp^2 \approx 1$, the exponential takes care of resumming many gluon exchanges, in a Glauber-inspired way. Intuitively, this is what happens when the proton starts to look dark. It is important to emphasize that one moves towards the unitarity bound for large $r_\perp$ in this saturation model much faster than that predicted by the CGC approach. However, as our goal is the charm production, which is dominated by the color transparency regime, the difference among the approaches can be disregarded in what follows. The saturation model depends upon the variables x and $r_\perp$ only through the dimensionless quantity $Q_{\text{sat}} r_\perp$. Consequently, the saturation model predicts the geometric scaling of the total cross section.

We are interested in the charm production in deep inelastic scattering. From the experimental point of view, the DESY ep collider HERA experiments have published data for the contribution of charmed meson production to the structure function F_2. Their analyses were based on D^0 and D^* meson tagging. This allows one to single out the charm contribution F_2^c to the total structure function and thus to investigate if the property of geometric scaling is also present in this observable. Before presenting our results, let us perform a qualitative analysis of the inclusive charm production using the saturation model [18] in order to shed light on the dipole configurations dominating the process in the relevant kinematical limits and show how the geometric scaling comes out. A characteristic feature in heavy quark production within the color dipole approach is that the process is dominated by small size dipole configurations [28]. The overlap function weighting the dipole cross section is peaked at $r_\perp \sim 1/m_c \simeq 0.1$ fm even for sufficiently low Q^2 values. As a consequence, charm production is dominated by color transparency and saturation effects are not important there, i.e., $\sigma_{\text{dip}} \simeq S_0(x, r_\perp) \equiv \sigma_0 Q_{\text{sat}}^2(x) r_\perp^2/4$, which is the leading order term in the expansion of S for small $r_\perp$. We consider for simplicity the transverse contribution, whose corresponding wave function is given by Eq. (1), and taking its asymptotic behavior at $\varepsilon r_\perp \ll 1$ such that $K_1(\varepsilon r_\perp) \sim 1/\varepsilon r_\perp$. This imposes an additional constraint to the z integration, namely, the integrand should be multiplied by the Heaviside function $\Theta(1 - \varepsilon^2 r_\perp^2)$; then

$$\sigma_T^c \sim \int_0^{4/(Q^2 + \mu_c^2)} \frac{dr_\perp^2}{r_\perp^2} S_0(x, r_\perp)$$
$$+ \int_{4/(Q^2 + \mu_c^2)}^{4/\mu_c^2} \frac{dr_\perp^2}{r_\perp^2} \left(\frac{1}{Q^2 r_\perp^2}\right) S_0(x, r_\perp), \qquad (4)$$

where $\mu_c^2 = 4m_c^2$. The first term corresponds to the symmetric dipole configurations, i.e., $\langle z \rangle \approx 1/2$, whereas the second term comes from aligned jet configurations, with the charm mass introducing a cutoff on the maximal size of the charmed dipole.

For the DESY ep collider HERA kinematical region, we have $Q_{\text{sat}}^2 \approx 1$ GeV^2, which implies that the relation $Q_{\text{sat}}^2 < Q^2 + \mu_c^2$ is ever satisfied. Consequently, we can define two kinematical regimes depending on the relation between Q^2 and μ_c^2. For $Q^2 \gg \mu_c^2$ we have scaling with logarithmic enhancement coming from aligned jet configurations, whereas for $Q^2 \ll \mu_c^2$ only symmetric dipole configurations contribute. Therefore, we obtain that

$$\sigma_T^c \sim \frac{\sigma_0 Q_{\text{sat}}^2(x)}{Q^2}\left(1 + \ln\frac{Q^2}{\mu_c^2}\right)\Theta(Q^2 - \mu_c^2)$$
$$+ \frac{\sigma_0 Q_{\text{sat}}^2(x)}{\mu_c^2}\Theta(\mu_c^2 - Q^2), \qquad (5)$$

where the first term provides the behavior $1/\tau$ at large τ, whereas the second term leads to a smooth transition down to the asymptotic (τ-independent) behavior at small τ.

An analytical expression for the τ dependence of the inclusive charm production can also be obtained in a less model dependent way. For this purpose we make use of the symmetric saturation model [26], where the energy evolution of the proton leads to the parton multiplication and the transverse momentum scale $Q_{\text{sat}}(x)$ appears. The main assumption is that the evolved proton can be described by a collection of independent dipoles at the time of the interaction whose sizes are distributed around $1/Q_{\text{sat}}$. The rate of growth of the parton densities is assumed to be $Q_{\text{sat}}^2(x)/\Lambda^2$ and the symmetry between low and high virtualities in γp interactions comes from the symmetry in the dipole-dipole cross section. The approach provides a quite intuitive and simplified expression for the inclusive production. Following such an approach, we obtain that in the DESY ep collider HERA kinematical regime, i.e., $Q_{\text{sat}}^2 < \mu_c^2$, the inclusive charm production is given by

$$\sigma_{\text{tot}}^c(\tau) = \frac{N_{c\bar{c}}}{\Lambda^2 \, \nu_>}\left\{1 - \exp\left[-\frac{\nu_>}{\tau + \tau_c}[1 + \log(\tau + \tau_c)]\right]\right\},$$

where $\tau_c = \mu_c^2/Q_{\text{sat}}^2(x)$ and the parameters are taken from the data fit in Ref. [26]. Here, we make the simplified assumption that the coupling with the dipole is flavor blind, in such a way that $N_{c\bar{c}} = (2/5)N$, with N being the global normalization describing F_2 data. The factor 2/5 corresponds to the charge fraction $e_c^2/(\sum e_{u,d,s}^2 + e_c^2)$. Once the parameters are fitted to proton structure function data, our prediction for the τ dependence in the inclusive charm production is parameter free. Moreover, the expression above gives an analytical result for the whole τ domain.

Results.—In Figure 1 we show the experimental data [29] on the total cross section for the inclusive charm production plotted versus scaling variable $\tau = Q^2/Q_{\text{sat}}^2$, with Q_{sat} from the saturation model. We include all available data covering the range $1.5 \leq Q^2 \leq 130$ GeV^2 [29]. It should be stressed that some bins with $x \geq 10^{-2}$ have
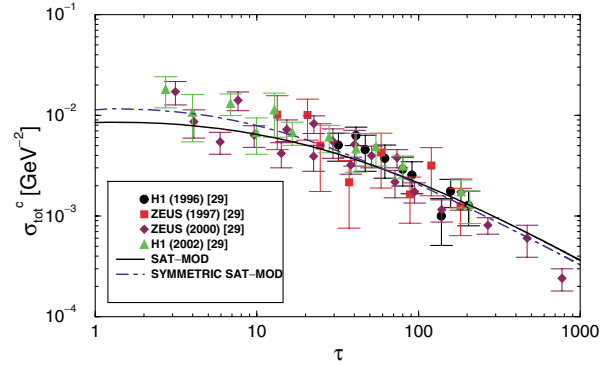

FIG. 1 (color online). Experimental data on inclusive charm production plotted versus the scaling variable $\tau = Q^2/Q_{\text{sat}}^2$.

also been included and old measurements contain somewhat large uncertainties. Moreover, charm data are influenced by a significant systematic uncertainty coming from the theoretical models used in the extraction of $F_2^{c\bar{c}}$. The combination of these factors produces a larger data dispersion than in the inclusive structure function. We see the data exhibit geometric scaling for the whole Q^2 range, verifying a transition in the behavior on τ of the cross section from a smooth dependence at small τ and an approximated $1/\tau$ behavior at large τ. The transition point is placed at $\mu_c^2 = 4m_c^2$, which takes values of order 10 GeV^2 for a charm mass $m_c = 1.5$ GeV. This turns out in $\tau \simeq 10$ since at the DESY ep collider HERA $Q_{\text{sat}}^2 \simeq 1$ GeV^2. The asymptotic $1/\tau$ dependence reflects the fact the charm production cross section scales as Q_{sat}^2/Q^2 modulo a logarithmic correction $\sim \ln(Q^2/\mu_c^2)$, with energy dependence driven by the saturation scale. The mild dependence at $\tau \lesssim \mu_c^2$ corresponds to the fact that the cross section scales as Q_{sat}^2/μ_c^2 towards the photoproduction limit, but with the same energy behavior given by the saturation scale. As also plotted in Fig. 2, we also found a symmetry between the regions of large and small τ for the function $\sqrt{\tau}\sigma_{\text{tot}}^c$ with respect to the transformation $\tau \leftrightarrow 1/\tau$ in the whole region of τ. The features present in the inclusive charm production data can be well reproduced in the phenomenological saturation model as
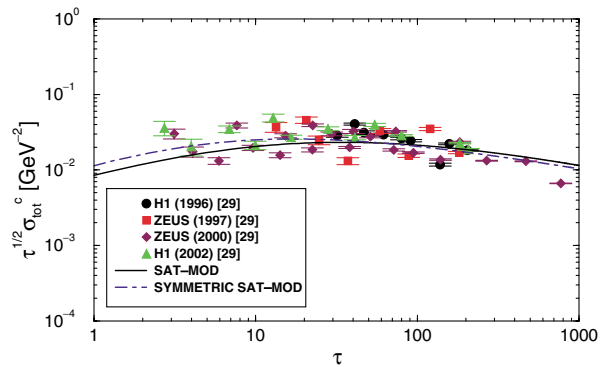

FIG. 2 (color online). The quantity $\sqrt{\tau}\sigma_{\text{tot}}$ plotted versus the scaling variable τ.

shown in Eq. (5), corresponding to the solid curve in Figs. 1 and 2. The symmetric saturation model also provides similar results, as shown in the dot-dashed lines. Disregarding the Glauber-like resummation in this model, the expression gets simplified to $\sigma_{\text{tot}}^c \propto \frac{1}{\tau+\tau_c} \times [1 + \log(\tau + \tau_c)]$, and the symmetric pattern is easily verified. Moreover, it is important to emphasize that a reasonable description of the charm photoproduction experimental data, which corresponds to $\tau = 0$, is also obtained using the symmetric saturation model. Our results for the nuclear heavy quark photoproduction indicate that similar behavior is expected in the nuclear case [30].

Summary.—Summarizing our results, one shows that the inclusive charm production exhibits geometric scaling in a large region of photon virtualities. In the DESY *ep* collider HERA kinematic domain the saturation momentum $Q_{\text{sat}}^2(x)$ stays below the hard scale $\mu_c^2 = 4m_c^2$, implying that charm production probes mostly the color transparency regime and saturation corrections are not very important. In the color dipole picture, the transition at $Q^2 \simeq \mu_c^2$ is related to the presence of aligned jet configurations at $Q^2 \gg \mu_c^2$ and complete dominance of symmetric configurations at $Q^2 \ll \mu_c^2$. An analytical result on the τ behavior was obtained within the symmetric saturation model, relying on quite simple assumptions about the dipole-proton interaction. An outstanding feature is the scaling on τ above the saturation scale, supported by recent theoretical formulations.

———

*Electronic address: barros@ufpel.tche.br
†Electronic addresses: magnus@if.ufrgs.br
magnus@ufpel.edu.br

[1] V. N. Gribov and L. N. Lipatov, Sov. J. Nucl. Phys. **15**, 438 (1972); G. Altarelli and G. Parisi, Nucl. Phys. **B126**, 298 (1977); Yu. L. Dokshitzer, Sov. Phys. JETP **46**, 641 (1977).

[2] L. N. Lipatov, Sov. J. Nucl. Phys. **23**, 338 (1976); E. A. Kuraev, L. N. Lipatov, and V. S. Fadin, JETP **45**, 1999 (1977); I. I. Balitskii and L. N. Lipatov, Sov. J. Nucl. Phys. **28**, 822 (1978).

[3] M. Froissart, Phys. Rev. **123**, 1053 (1961); A. Martin, Phys. Rev. **129**, 1432 (1963).

[4] L. V. Gribov, E. M. Levin, and M. G. Ryskin, Phys. Rep. **100**, 1 (1983).

[5] A. H. Mueller and Jian-wei Qiu, Nucl. Phys. **B268**, 427 (1986).

[6] J. Bartels, Z. Phys. C **60**, 471 (1993); **62**, 425 (1994); J. Bartels and M. Wüsthoff, Z. Phys. C **66**, 157 (1995); J. Bartels and C. Ewerz, J. High Energy Phys. **09** (1999) 026.

[7] L. McLerran and R. Venugopalan, Phys. Rev. D **49**, 2233 (1994); **49**, 3352 (1994); **50**, 2225 (1994).

[8] E. Iancu, A. Leonidov, and L. McLerran, Nucl. Phys. **A692**, 583 (2001); E. Ferreiro, E. Iancu, A. Leonidov, and L. McLerran, Nucl. Phys. **A701**, 489 (2002).

[9] A. L. Ayala Filho, M. B. Gay Ducati, and E. M. Levin, Nucl. Phys. **B493**, 305 (1997); **B511**, 355 (1998).

[10] I. I. Balitsky, Nucl. Phys. **B463**, 99 (1996); Phys. Rev. Lett. **81**, 2024 (1998); Phys. Rev. D **60**, 014020 (1999); Phys. Lett. B **518**, 235 (2001); I. I. Balitsky and A. V. Belitsky, Nucl. Phys. **B629**, 290 (2002).

[11] J. Jalilian-Marian, A. Kovner, L. McLerran, and H. Weigert, Phys. Rev. D **55**, 5414 (1997); J. Jalilian-Marian, A. Kovner, and H. Weigert, Phys. Rev. D **59**, 014014 (1999); **59**, 014015 (1999); **59**, 034007 (1999); A. Kovner, J. Guilherme Milhano, and H. Weigert, Phys. Rev. D **62**, 114005 (2000); H. Weigert, Nucl. Phys. **A703**, 823 (2002).

[12] Y. V. Kovchegov, Phys. Rev. D **60**, 034008 (1999); **61**, 074018 (2000).

[13] E. M. Levin and K. Tuchin, Nucl. Phys. **B573**, 833 (2000); Nucl. Phys. **A691**, 779 (2001); **A693**, 787 (2001).

[14] M. A. Braun, Eur. Phys. J. C **16**, 337 (2000); N. Armesto and M. A. Braun, Eur. Phys. J. C **20**, 517 (2001).

[15] E. Gotsman, E. M. Levin, M. Lublinsky, and U. Maor, Nucl. Phys. **A696**, 851 (2001); M. Lublinsky, Eur. Phys. J. C **21**, 513 (2001).

[16] K. Golec-Biernat, L. Motyka, and A. M. Stasto, Phys. Rev. D **65**, 074037 (2002); K. Golec-Biernat and A. M. Stasto, Nucl. Phys. **B668**, 245 (2003).

[17] A. H. Mueller and D. N. Triantafyllopoulos, Nucl. Phys. **B640**, 331 (2002); D.N. Triantafyllopoulos, Nucl. Phys. **B648**, 293 (2003); A. H. Mueller, Nucl. Phys. **A724**, 223 (2003).

[18] K. Golec-Biernat and M. Wüsthoff, Phys. Rev. D **59**, 014017 (1999); **60**, 114023 (1999).

[19] J. Bartels, K. Golec-Biernat, and H. Kowalski, Phys. Rev. D **66**, 014001 (2002).

[20] H. Kowalski and D. Teaney, hep-ph/0304189 [Phys. Rev. D (to be published)].

[21] E. Iancu, K. Itakura, and L. McLerran, Nucl. Phys. **A708**, 327 (2002).

[22] J. Kwiecinski and A. M. Stasto, Phys. Rev. D **66**, 014013 (2002).

[23] A. M. Staśto, K. Golec-Biernat, and J. Kwieciński, Phys. Rev. Lett. **86**, 596 (2001).

[24] S. Munier and S. Wallon, Eur. Phys. J. C **30**, 359 (2003).

[25] A. Freund, K. Rummukainen, H. Weigert, and A. Schafer, Phys. Rev. Lett. **90**, 222002 (2003).

[26] S. Munier, Phys. Rev. D **66**, 114012 (2002).

[27] V. Barone and E. Predazzi, *High-Energy Particle Diffraction* (Springer-Verlag, Berlin, Heidelberg, 2002).

[28] N. N. Nikolaev and V. R. Zoller, Phys. Lett. B **509**, 283 (2001).

[29] H1 Collaboration, C. Adloff *et al.*, Z. Phys. C **72**, 593 (1996); ZEUS Collaboration, J. Breitweg *et al.*, Phys. Lett. B **407**, 402 (1997); ZEUS Collaboration, J. Breitweg *et al.*, Eur. Phys. J. C **12**, 35 (2000); H1 Collaboration, C. Adloff *et al.*, Phys. Lett. B **528**, 199 (2002).

[30] V. P. Goncalves and M. V. Machado, Eur. Phys. J. C **30**, 387 (2003).